Communications in **M**athematical **A**nalysis
Volume 17, Number 2, pp. 34–44 (2014) www.math-res-pub.org/cma
ISSN 1938-9787

Heuristic Approach to Study the Optimal Path of the Light Emission in a Percolating Cluster

Yessica Yazmin Calderón-Segura*
Centro de Investigación en Ingeniería y Ciencias Aplicadas
Universidad Autónoma del Estado de Morelos,
Cuernavaca, Mor. 62209, México.

Gennadiy Burlak†
Centro de Investigación en Ingeniería y Ciencias Aplicadas
Universidad Autónoma del Estado de Morelos,
Cuernavaca, Mor. 62209, México.

(Communicated by Vladimir Rabinovich)

Abstract

In this paper a porous 3D system wherein the material porosity forms a percolating spanning cluster is studied. It is considered that the light nanoemitters are randomly incorporated into such a cluster and are pumped to the exited state by an external light beam. To find the optimal optical path between the radiated nanoemitters the Fermat principle was used and it is implemented by means of well-known the travelling salesman (TSP) approach generalized to 3D geometry. With the use of undirected graph mapping the TSP approach is applied for optimizing optical path (for principle of Fermat) to calculate the optimal light paths in such a percolation structure. The convergence of the algorithm for 3D incipient cluster is studied with details to exploit the space of feasible solutions when a collective light radiation of the internal nanoemitters becomes. Finally, the field correlations of the light emission that penetrates the entire 3D percolation cluster is discussed.

AMS Subject Classification: 65N25; 74J05; 78A25; 78A40.

Keywords: Percolation, optimization, nanoemitters, numerical calculations.

1 Introduction

In the inhomogeneous nanostructures the optical nanoemitters (quantum dots, etc.) communicate by means of optical radiation that allows the field correlations and leads to various

*E-mail address: ycalderons@uaem.mx
†E-mail address: gburlak@uaem.mx

collective interactions between such nanoobjects, see e.g. [1]-[3] and references therein. The ordering and the details of field's communication normally require the knowledge of the optimal optical path (length) between the emitters. In general the definition of optimal path is an advanced problem for structures with large number of emitters. The principle of Fermat, known also as the principle of the shortest optical path, asserts that the optimal optical path S between any two points $\mathbf{r}_0$ and $\mathbf{r}_1$ (n_r is the refraction index of medium) reads

$$S = \int_{\mathbf{r0}}^{\mathbf{r1}} n_r ds = \min \tag{1.1}$$

for an actual ray that is shorter than the optical length of any other curve which joins these points [4]. In place of such variational problem different approaches to the path optimization can be offered. We refer here to the Traveling Salesman Problem (TSP) that is probably is one of the best studied optimization problem [5] - [16]. Such a problem is formulated as searching the shortest path of a traveling agent who starts from a destination city, has to visit a number of default and return back to the starting city. The path obviously depends on the order in which the agent visit the cities. It is worth noting that TSP is NP-complete problem [14]: for a complete undirected graph on n vertices the size of the search space is $(n-1)!/2$ [15]. In the literature it is used various approaches, e.g. exact techniques as meta-heuristics and heuristics, and also the optimized annealing of TSP (Metropolis algorithm, e.g. [17]) from the n-th nearest-neighbor distribution [18]. Solving TSP is based on an adaptive simulated annealing algorithm with greedy search [19]. SOM-based particle matching algorithm for 3D particle tracking velocimetry was studied in Ref.[20].

For the optical context of this problem it is worth noting the following. Whereas the output beam of a laser has a linear polarization [4]-[26], an algorithmic solution approach can be implemented as finding a Hamiltonian cycle of lower cost with the use of a undirected graph. To check the convergence of such algorithm we have implemented it for radiated nanoemitters integrated in 3D percolating porous ceramic. This paper is organized as follows: In Section II we describe the problem to solve. In Section III, we present the mathematical model that is more specified in Sec. IV. In Sec. V we study the spectral distribution of the nanoemitter's field correlations. In the last Section, we summarize our results and conclusions.

2 Description of the problem

We consider that a porous material can be represented by 3D reference grid. The porosity is generated randomly with occupation probability p and for critical probability p_c such that $p \geq p_c$ a spanning percolating cluster emerges. If the grid has at least two pores the latter will communicate only if the distance between them is less than the sum of radiuses that allows generating a simple percolating cluster. After formation of the spanning cluster at $p \geq p_c$, the opportunity to incorporate the nanoemitters through such the opened cluster structure becomes possible. The cross-section of clusters normally exceeds the field wavelength; therefore, such a network forms the open waveguide system by means of which the passage of the intensive laser pulse behaves as the field pump. As a result, the two-level nanoemitters incorporated into spanning cluster will be raised to the excited state. For

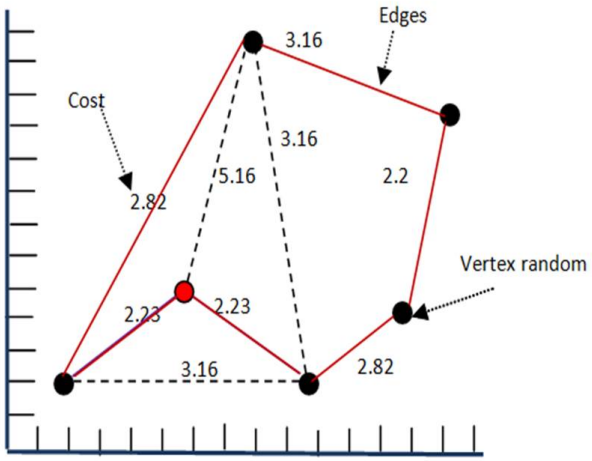

Figure 1. Weighted clique type non-directed graph

simplification of the problem, we have used the natural assumption that nanosources are incorporated only in those clusters which have a connection with the entrance (input for laser pump) side of the sample. The analysis of such a system consists of two steps, and in general it requires quite long computation [25].-[28] The first step deals with identification of the spanning cluster P_s as a function of probability p. In the second step, the field properties of radiating nanoemitters incorporated into the percolation structure (known from the first step) are calculated with the use of technique FDTD [29]. To define the optimal optical path of the pump beam we will map such a problem to the traveler problem (TSP) where all the nanoenitters serve as cities to be visited. With such analogy one can simplify the optical problem to well-known optimization problem (TSP) when the set of n nanoemitters will be represented by n cities, $V = \{1, 2, 3 \ldots, n\}$. Finally the optimal path calculated from TSP will correspond to the shortest optical path of the laser beam that fits the Fermat principle. Corresponding graphical representation is defined as a graph G and a set of edges E, belonging to the graph, where $E(G)$ are not ordered pairs of elements and another set of nodes (pores) V belongs to the graph $G(V, E)$ [20]-[23].

Figure 1 shows the representation of the problem of agent traveller in a symbolic way in a non-direct graph, by setting the distance for each node with the use the equation Eq.(3.1)**.**

The symbolic representation of the non-directed graph, is shown in Figure 2, where the penetration of laser beam through the pores which form the percolating cluster in the porous material. In this case the optical beam penetrates the system and all possible trajectories are represented by vertices and edges that symbolize the non-directed graph. This representation shows the cost of propagating between two pores when beam percolates a sample with a small fragment of represented light. Thus the dotted points in five nodes will represent the reflected light. The best trajectory of the reflected light becomes as the

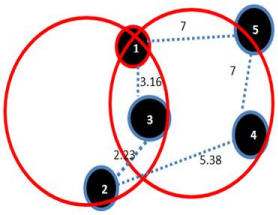

Figure 2. Representation of the cost in two pores

following: $\{1-3, 3-2, 2-4, 4-5, 5-1\}$ (see figure 2)

3 The model

To find the solution to TSP in a porous structure, we generated a graph representing the pores in the system. Is the graph $G(V,E)$ are defined the vertices $V = \{1,\ldots,n\}$, and E represents the edges. In this way the problem of traveler is to find a route (Hamiltonian cycle) in G in which the sum of the preserves of the edges or connections of the route is small as possible. It is assumed that G is a complete graph.

This task considers an array of weights representing the costs (distances) between each city (pores), such matrix is defined as $C(C_{ij})_{nxn}$ where the value (i, j) corresponds to the C_{ij} which is the cost or distance to join a node (pore) i with the node j in G. is shown in Figure 1. According to this is the mathematical formulation for the agent reads.

$$Min \quad z(x) = \sum_{(i,j)\in A} c_{ij}x_{ij}, \tag{3.1}$$

subject to

$$\sum_{\{i:(i,j)\in A\}} x_{ij} = 1, \forall j \in V, \tag{3.2}$$

and

$$\sum_{\{j:(i,j)\in A\}} x_{ij} = 1, \forall j \in V, \tag{3.3}$$

and

$$\sum_{\{(i,j)\in A: i\in U, J\in(V-U)\}} x_{ij} > 1, 2 < |U| < |V| - 2, \tag{3.4}$$

where Eq. (3.1) corresponds to the objective function calculation. The restriction (3.2) indicates that the beam of light can visit every emitter once in each cycle of travel, here x_{ij} denotes the value of cost of the euclidean distance between i the j nanoemitters. The restriction (3.3) indicates that since pore j can pass to a unique pore i and exit by a single road. The condition (3.4) prevents the generation of subtours.

4 Adaptation of the optimization technique

Initially a feasible solution and a possible solution that improves the initial one is generated with the help of a search by neighborhood. Such a search encods the cities (the pores) and the path of the incident beam in the medium. We use here the technique of simulated annealing optimization tailored to the problem of agent traveller. In such approach a random change in the path is generated to improve the initial solution with E, where $E = |r1 - r0|$ for some trial $r1, r0$ in the path. If generated new state has a lower energy than the previous state such that $E = 0$, this new state is taken to the next iteration. Otherwise, if generated new state has that $E > 0$ this one is accepted with a Gaussian probability that depends on some parameter T_0 (temperature). With the increases of the iteration the simulated annealing algorithm shows the convergence of the TSP model to the optimal solution in the percolation cluster. The process runs as follows: (i) defines the dimension of the 3D grid with a pore size and distance between pores as well as the critical probability p_c to form a percolation cluster (see Figure 2), (ii) then the system randomly generates a path of light beam between the pores with a specific weight W_{ij}, (iii) if $p > p_c$, the system generates a percolation cluster that will be analyzed with the use of an undirected graph. This results that the optical beam penetrates through the all network. The implementation of such algorithm (pseudocode) is presented as follows

Requires: Initialize array of weights $W_{i,j}$for every ray of light in every pore
  While the weights $W_{i,j}$ and the distance between them is less than your radius
    For each node V_i in $G(V,E)$ do
      Present Vi pore network
      Obtain the cluster connection
      If $p_c < p$ then
        Random value is generated
        If $p_c > p$ then
          Create cluster
          Assign weight for each pore $W_{i,j}$
        If not
          Generate p_c
    End if
  End for
  Upgrade path from the neighborhood radius laser beam

End while.

5 The spectral distribution of the field correlations

The above discussed method of simulated annealing (see e.g. [17] and references therein) is a technique that has attracted significant attention as suitable for optimization problems of large scale, especially ones where a desired global extremum is hidden among many, poorer, local extrema. In this Section we apply this method to find the minimal optical path that (following the Fermat principle) links the nanoemitters incorporated in the percolating cluster. The calculated typical path is shown in Fig.3 as a solid line.

In what follows we will calculate the spectral distribution of the field correlation (fluctuation) function for the nanoemitters incorporated in the percolating cluster having fixed frequency ω at some temperature T. We assume that the emitters already are ordered in a shortest optical path. By expressing the correlation functions of the electromagnetic fluctuations in terms of the retarded Green's function D^R_{ik}, for non-magnetoactive media, such function can be written as [24]

$$\left\langle A_i^{(1)} A_k^{(2)} \right\rangle_{\omega,k} = -\coth(\hbar\omega/2T)\,\mathrm{Im}(D^R_{ik}(\omega; r_1, r_2)). \tag{5.1}$$

where $A_i^{(k)}$ is the vectorial potential in point r_k. In a homogeneous infinite medium, the Green functions $D^R_{ik}(\omega; r_1, r_2)$ depend only on the difference $r = r_2 - r_2$. In an isotropic non-magnetic ($\mu = 1$) medium from Eq.(5.1) one can obtain the following field correlation function

$$\left\langle \mathbf{E}^{(1)}\mathbf{E}^{(2)} \right\rangle_\omega = -2\hbar \cdot \coth(\frac{\hbar\omega}{2T})\,\mathrm{Im}\left\{ \frac{1}{\varepsilon}\left[\frac{\varepsilon\omega^2}{\mathbf{r}c^2} \exp(-\frac{\omega\varepsilon}{c}\sqrt{-\varepsilon}) + 2\pi\delta(\mathbf{r}) \right] \right\}. \tag{5.2}$$

where $r = |r_2 - r_1|$ and $\sqrt{-\varepsilon}$ is to be taken with the sign that makes $\mathrm{Re}(\sqrt{-\varepsilon}) > 0$; for a vacuum we must put $\varepsilon = 1$, $\sqrt{-\varepsilon} = -i$ [24].

The occurrence of the imaginary part of in Eq.(5.2) shows clearly the relation between the electromagnetic fluctuations and the absorption in the medium. But if to take the limit $\mathrm{Im}(\varepsilon) \to 0$ in these expressions, one obtains non-zero results [24]. This is connected with the order in which two limits are taken, those of an infinite medium and zero $\mathrm{Im}(\varepsilon)$. Since in an infinite medium an arbitrarily small $\mathrm{Im}(\varepsilon)$ eventually gives rise to absorption, with our order of taking the limits the result pertains to a physically transparent medium in which, as in any actual medium, there is still some absorption. For example, let us take these limits in Eq.(5.2). To do that we note that for a small positive $\mathrm{Im}(\varepsilon)$ (with $\omega > 0$) we have $\sqrt{-\varepsilon} \approx -i\sqrt{\mathrm{Re}(\varepsilon)}(1 + i\frac{\mathrm{Im}(\varepsilon)}{\mathrm{Re}(\varepsilon)})$ (using the condition that $\mathrm{Re}(\varepsilon) > 0$). Hence, in the limit $\mathrm{Im}(\varepsilon) \to 0$, the correlation function read

$$\left\langle \mathbf{E}^{(1)}\mathbf{E}^{(2)} \right\rangle_\omega = \frac{1}{n^2}\left\langle \mathbf{H}^{(1)}\mathbf{H}^{(2)} \right\rangle_\omega = \frac{2\hbar\omega^2}{rc^2}\coth(\frac{\hbar\omega}{2T})\sin(\frac{\omega n r}{c}), \tag{5.3}$$

where $n = \sqrt{\varepsilon}$ is the real refractive index of the host medium. It is worth noting that this expression remains finite even when the points r_1 and r_2 coincide:

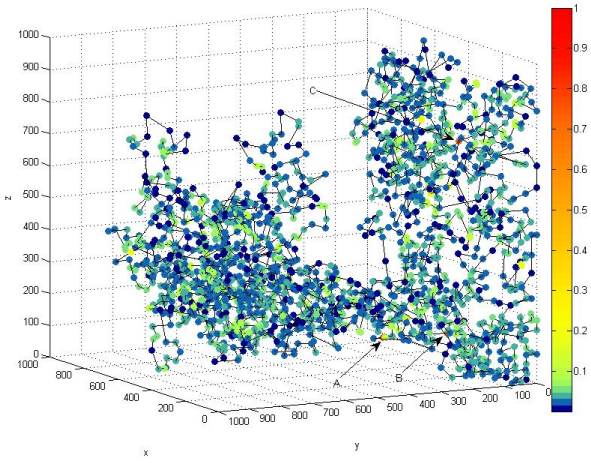

Figure 3. (Color on line.) The spectral distribution of field correlations (fluctuations) for nanoemitters in the optimal optical path for the percolating cluster in the transparent medium. Arrows A, B, and C indicate the points with the maximal values of the field correlations $\left\langle \mathbf{E}^{(1)}\mathbf{E}^{(2)}\right\rangle_{\omega}$, see Eq.(5.3). The solid curves show the optimal optical path (that agrees with the Fermat principle). See details in the text.

$$\left\langle \mathbf{E}^2\right\rangle_{\omega} = \frac{1}{n^2}\left\langle \mathbf{H}^2\right\rangle_{\omega} = \frac{2\hbar\omega^3 n}{c^3}\coth(\frac{\hbar\omega}{2T}). \tag{5.4}$$

In what follows we calculate the spatial distribution of the field's correlation in Eq. (5.3) through the all optical path to study the strength of the field correlations between the nearest nanosources. The typical result of simulations is shown in Fig. 3.

Fig. 3 shows the spectral distribution of the field correlations (fluctuations) of nanoemitters situated in the optimal optical path in the percolating cluster for the transparent medium. Arrows A, B, and C indicate the points with maximal value of the field correlations $\left\langle \mathbf{E}^{(1)}\mathbf{E}^{(2)}\right\rangle_{\omega}$, see Eq.(5.3). The solid curves show the optimal optical path. From Fig. 3 we observe that the level of field's correlations strongly depends on the position of nanoemitter.

In a transparent medium Eq.(5.3) also can be written in $\mathbf{k}$-space in the following form

$$\left\langle E_i^{(1)}E_k^{(2)}\right\rangle_{\omega,\mathbf{k}} = \frac{2\pi\hbar^2}{k}(\frac{\omega^2}{c^2}\delta_{ik} - \frac{k_i k_k}{n^2})\{\delta(\frac{\omega n}{c} - k) - \delta(\frac{\omega n}{c} + k)\}\coth(\frac{\hbar\omega}{2T}) \tag{5.5}$$

The arguments of the delta functions in Eq.(5.5) have a simple physical meaning: they show that the field correlations with a given value of $\mathbf{k}$ are propagated in space with velocity c/n, equal to that of propagation of electromagnetic waves in the same medium.

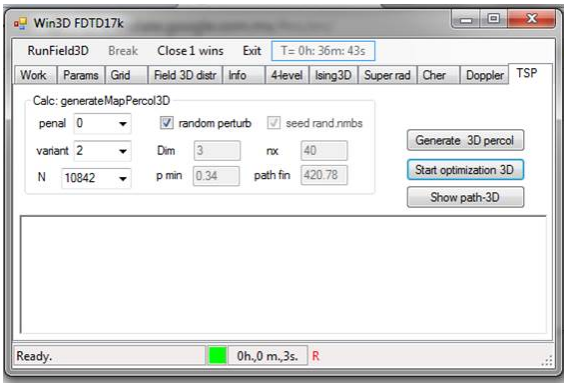

Figure 4. Program that generates the simulation of porous material

6 Results and discussion

We investigated the problem of the simulating 3D field structure of nanoemitters numerically. Our results are shown in Fig. 3. We have implemented a configuration of random nodes and simulated the path of the beam laser using the Fermat principle with the use of traveller agent problem approach. The program code was executed on a PC with an Intel Core processor i7-740QM quad processor (1. 73GHz) with Turbo Boost up to 2.93GHz based on Windows 7 Home Premium 64-bit operating system. It is used the compiler Visual C# 2013. Figure 4 shows the program that generates the simulation of porous material, defining the size and distance of pore, the size of the array to work, likely critical p_c to determine the porosity in the system and a number of nanoemitters issued by the laser beam, which which was optimized in this simulation.

Figure 4 shows the first generated solution when they penetrate the laser beam on the porous material, in this same solution the best trajectory of the laser beam is generated through the agent problem traveller. shows the convergence of the algorithm implemented in a critical probability of 0.34 on duration 36 m:43 seconds. The algorithm checked that the optimal way of 10842 nanoemitters incorporated in a porous ceramics. In this case the normalized length of the optimal pass was 420.73.

7 Conclusions

We studied a porous 3D system wherein the material porosity forms a percolating spanning cluster. It is considered that the light nanoemitters are randomly incorporated into such a cluster and are pumped to the exited state by an external light beam. To find the optimal optical path between the radiated nanoemitters the Fermat principle was used and it is implemented by means of well-known the travelling salesman (TSP) approach generalized to 3D geometry. With the use of undirected graph mapping the TSP approach is applied for optimizing optical path (for principle of Fermat) to calculate the optimal light paths in such a percolation structure. The convergence of the algorithm for 3D incipient cluster is studied with details to exploit the space of feasible solutions when a collective light radiation of the internal nanoemitters becomes. The field correlations of the light emission that penetrates the entire 3D percolation cluster is studied also.

8 Acknowledgments

This work was partially supported by CONACyT (México) grants No. 169496, No. 168104, No. 246220 (Sabbatic), and project Redes de PROMEP (México).

References

[1] Lei Wang, Shou-Jun Zhu, Hai-Yu Wang, Song-Nan Qu, Yong-Lai Zhang, Jun-Hu Zhang, Qi-Dai Chen, Huai-Liang Xu, Wei Han, Bai Yang, and Hong-Bo Sun, Common Origin of Green Luminescence in Carbon Nanodots and Graphene Quantum Dots. *ACS Nano* **8** (2014), pp 2541-2547.

[2] Sahin Derya, Ilan Boaz, and Kelley David F, Monte-Carlo simulations of light propagation in luminescent solar concentrators based on semiconductor nanoparticles. *Journal of Applied Physics.* **110** (2011), pp 033108.

[3] Xiaoming Wen, Pyng Yu, Yon-Rui Toh, Xiaoqian Jau Tang, On the upconversion fluorescence in carbon nanodots and graphene quantum dots. *Chem. Commun.* **50** (2014).

[4] M. Born and E. Wolf, *Principles of Optics, Pergamon*, Edition 7th, 1980, pp 1-936.

[5] Irene Charon and Olivier Hudry, Application of the noising method to the travelling salesman problem. *European Journal of Operational Research*. **125** (2000), pp 266-277.

[6] Adam N. Letchford, Saeideh D. Nasiri, and Dirk Oliver Theis, Compact formulations of the Steiner Traveling Salesman Problem and related problems. *European Journal of Operational Research*. **228** (2013), pp 83-92.

[7] Erasmo Lopez, Oscar Salas, and Alex Murillo, El problema del Agente Viajero: Un algoritmo deterministico usando busqueda tabu. *Revista de Matematicas y Aplicaciones* (2014) (1), pp 127-144.

[8] Hsuan-Ming Feng and Kuo-Lung Liao, Hybrid evolutionary fuzzy learning scheme in the applications of traveling salesman problems. *Information Sciences*. **270** (2014), pp 204-225.

[9] Michael Bass, *Handbook of Optics Fundamentals*, Techniques & Design, Second Edition Volume, 1997.

[10] Hsuan-Ming Feng and Kuo-Lung Liao, Hybrid evolutionary fuzzy learning scheme in the applications of traveling salesman problems. *Information Sciences* **270** (2014), pp 204-225.

[11] J. Majumdar and A. K. Bhunia, Genetic algorithm for asymmetric traveling salesman problem with imprecise travel times. *Journal of Computational and Applied Mathematics* **235** (2011), pp 3063-3078.

[12] Shlomi Dolev and Hen Fitoussi, Masking traveling beams: Optical solutions for NP-complete problems, trading space for time.*Theoretical Computer Science* **411** (2010), pp 837-853.

[13] Manabu Hasegawa and Kotaro Hiramatsu, Mutually beneficial relationship in optimization between search-space smoothing and stochastic search. *Physics A*, **392** (2013), pp 4491-4501.

[14] Maria Teresa Godinho, Luis Gouveia and Pierre Pesneau, Natural and extended formulations for the Time-Dependent Traveling Salesman Problem. *Discrete Applied Mathematics* **164** (2014), pp 138-153.

[15] Vikrant Vig and Udatta S. Palekar, On estimating the distribution of optimal traveling salesman tour lengths using heuristics. *European Journal of Operational Research* **18** (2008), pp 111-119.

[16] Christos H. Papadimitriou and Kenneth Steiglitz, *Algorithm to inverse problem of one-dimensional coupled radiation and conduction heat transfer Combinatorial optimization algorithms and complexity*, Prentice Hall 1982.

[17] William H.Press, Saul A. Teukovsky, William T. Vetterling, and Brian P. Flannery, *Numerical recipes in C++*. University Press, Cambridge 2002.

[18] Xiutang Geng, Zhihua Chen, Wei Yang, Deqian Shi, and Kai Zhao, Solving the traveling salesman problem based on an adaptive simulated annealing algorithm with greedy search. *Applied Soft Computing* **11** (2011), pp 3680-3689.

[19] Ahoy Ghatak and K. Thyagarajan, *Introduction to fiber optics*, New Dalhi, March 1997.

[20] Yessica Yazmin Calderon-Segura and Marco Antonio Cruz-Chavez, Estructura Hibrida de Vecindad para el Problema del Emparejamiento de Peso Maximo. *CICos* (2011), pp 72-82.

[21] Yong Chen and Pan Zhang, Optimized annealing of traveling salesman problem from the nth-nearest-neighbor distribution. *Physica A* **371** (2006), pp 627-632.

[22] Kazuo Ohmi, SOM-Based particle matching algorithm for 3D particle tracking Velocimetry. *Applied Mathematics and Computation* **205** (2008), pp 890-898.

[23] M. A.Cruz-Chavez, Diaz-Parra O., Juarez Romero D., Barreto Sedeco E., Zavala Diaz C., and Martinez Rangel M. G., Un Mecanismo de Vecindad con Busqueda Local y Algoritmo Genetico para Problemas de Transporte con Ventanas de Tiempo. *CICos 2008, 6to Congreso Internacional de Computo en Optimizacion y Software*, **60** 2008.

[24] E. M. Lifshitz and L. P. Pitaevskii, *Statistical Physics, Part 2*, Vol. 9, Pergamon, Oxford 1981.

[25] G. Burlak, A. Diaz-de-Anda, Yu. Karlovich, and A.B. Klimov, Critical behavior of nanoemitter radiation in a percolation material. *Phys. Lett. A*. **373** (2009), pp 1492-1500.

[26] Christos H. Papadimitriou and Kenneth Steiglitz, Algorithm to inverse problem of one-dimensional coupled radiation and conduction heat transfer. *Combinatorial optimization algorithms and complexity*, Prentice Hall 1982.

[27] G. Burlak, M. Vlasova, P. A. Marquez Aguilar, and L. Xixitla-Cheron, Optical percolation in ceramics assisted by porous clusters. *Opt. Commun* **282** (2009), pp 2850-2856.

[28] Yessica Calderon-Segura, Gennadiy Burlak, Martin G. Martinez-Rangel, Alberto Ochoa, and Alina Martinez-Oropeza, Percolationby links applied to the minimum spanning tree problem. *CONIELECOMP* (2013), pp 67-73.

[29] Allen Taflove and Susan C. Hagness, *Computational Electrodynamics: The Finite-Difference Time-Domain Method*, 3rd edition, Artech House Publishers 2005.